Journal of Imaging Science and Technology® 54(2): 020506–020506-9, 2010.

Robust Scheme for Detection of an Expanding Moving Object Using a Facet-Based Model in Infrared Imaging

Changhan Park
Samsung Thales Co. Ltd., Chang-Li 304, Namsa-Myun, Cheoin-Gu, Yongin, Gyeonggi 449-886, Korea

Hwal-Suk Lee
School of EECS, Korea Advanced Institute of Science and Technology, 373-1 Guseong-Dong, Yuseong-Gu, Daejeon 305–701, Korea

Jieun Kim
Agency for Defense Development, P.O. Box 35, Yuseong, Taejon 305-600, Korea

Kyung-Hoon Bae▲
Samsung Thales Co., Ltd., Chang-Li 304, Namsa-Myun, Cheoin-Gu, Yongin, Gyeonggi 449-886, Korea
E-mail: khbae.bae@samsung.com

Abstract. *In detection and tracking of a small or large moving object in infrared (IR) imaging systems, it is necessary to perform analysis of the object in real time. The authors proposed the facet-based detection scheme for a small moving object with zero-mean Gaussian noise in previous research. However, it is difficult to detect larger moving objects using the facet-based model because the kernel size in the facet-based model is* 5×5 pixels. *In this article, the authors propose a robust detection scheme using the facet-based model in IR for larger moving objects. A new condition for the object is proposed for the robust facet-based detection of a larger object with zero-mean Gaussian noise. In the proposed algorithm, first, we extract a mean of image intensity from the center of the facet in the region of interest (ROI) of the first frame. Second, we apply the facet-based model to the same positioned pixel in a subsequent frame. The pixels are detected from the maximum extreme condition. The pixels are detected from the maximum extreme condition. The experimental results show that the proposed algorithm is efficient and robust. © 2010 Society for Imaging Science and Technology.*
[DOI: 10.2352/J.ImagingSci.Technol.2010.54.2.020506]

INTRODUCTION

Infrared (IR) object detection and tracking are important functions of surveillance imaging systems on board military aircraft. The image and signal processing unit of the infrared search and tracking system detects and tracks approaching enemy missiles through intensive computation.[1] The high-speed IR detection and tracking system allows the capture of target movement and provides an image sequence that is essential for the analysis and evaluation of the threatening target. Preprocessing, object detection, feature extraction, object classification, and recognition in the IR imaging system are very important stages in image sequence processing and analysis.[2] Approaches developed for object detection can be roughly categorized into filtering-based, mapping-based, and feature-based. In filtering-based detection, various kinds of filters, spatial or temporal, are developed to suppress background clutter.[3] Passive detection of small targets embedded in IR image data is a difficult task. In order to achieve longer range performance, the system threshold sensitivity must be increased. Without improved clutter rejection techniques, increasing the system sensitivity will result in an unacceptable false alarm rate due to background clutter.[4]

Small and large moving object detection under unfavorable conditions is an important and difficult problem in real-time IR imaging systems. In mathematical morphology and motion analysis, namely, the moving point object detection method in IR or visual images,[5] the images are filtered by means of gray scale morphology in order to reject background clutter. Then, with the residual image, a motion analysis based on trajectory conjunction is carried out to extract the potential point-like moving objects. Through motion analysis, the nonobject points are eliminated. TopHat was proposed in a slowly small moving object detection method for use in an IR image.[6] The energy of the area around the location of an object often shows an intensity maximum or local energy maximum. The Butterworth high-pass filter (BHPF) method[7] and two-dimensional normalized least mean square (TDNLMS) method[8] have been presented as small object detection methods in IR imaging systems. The performances of BHPF and TDNLMS are good, but execution is time consuming, so they are not well suited for real-time systems.

The facet-based detection method applied the extreme theory for small object detection,[9] and Wang et al. presented robust conditions founded on facet-based detection.[10] A facet is defined as a region of interest (ROI) in an IR image

▲IS&T Member.

Received Feb. 25, 2009; accepted for publication Dec. 3, 2009; published online Feb. 26, 2010.
1062-3701/2010/54(2)/020506/9/$20.00.

sequence. The gray-level intensity distribution at each facet is approximated by a bivariate cubic polynomial basis through a linear combination of the intensity values.[11] We also presented the facet-based detection method for a small moving object with zero-mean Gaussian noise.[12] The performance of the facet-based detection method is good and efficient.

Noise, especially zero-mean Gaussian noise, happens in many IR imaging systems, and this noise affects the detection and tracking performances of an object. We presented the maximum extremum condition of the facet-based detection method to mitigate the noise in our previous research.[12]

The proposed scheme consists of two stages. First, we extract a mean of image intensity from the center of the facet in the ROI of the first frame. Second, we apply the facet-based model to the same-positioned pixel in a subsequent frame. If the size of the current object is larger than the previous object, it is divided into many objects to which the facet-based model is applied. Thus, the kernel size larger than 5×5 occurs because the facet-based model is modeling of a third order polynomial expression, which determines the limit of kernel size. Therefore, we propose a scheme that compares a mean of image intensity for 3×3, 5×5, and 7×7 from the center of the facet-based model kernel. The proposed scheme can extract not only one large object but also many objects.

SCHEME FOR MOVING OBJECT DETECTION

In this section, we present a brief overview of some object detection algorithms. A representative set of state of the art techniques was implemented and tested. A comparison was carried out and the conclusions are presented.

Frame Difference Analysis

The basic method to extract an object in an IR imaging system is frame difference analysis. This method can extract motion between the current object and a previous object but not if background clutter occurs. IR images can be filtered using frame difference, as follows:

$$I_{k-1}(x,y) - I_k(x,y) \geq 0, \tag{1}$$

where $I_{k-1}(x,y)$ and $I_k(x,y)$ represent previous frame and current frame, respectively.

Motion Analysis

A small moving object occupies merely one or several pixels in an IR image. It provides no information about intensity, size, shape, and velocity. However, a large moving object has lots of information about intensity, size, shape, and velocity. Motion is one of the most important cues for the detection of objects. The best motion cues regarding the object are extracted from the potential object by means of IR image filtering and motion analysis. The original IR image sequences are filtered using gray scale mathematical morphology. Then, a motion analysis based on trajectory conjunction is carried out on the residual image to extract potential point-like moving objects. IR images can be filtered using gray scale opening and closing, as follows:

$$Hyb(f) = (O_g(f) + C_g(f))/2, \tag{2}$$

where $O_g(f)=(f\circ g)\cdot g(x)$ and $C_g(f)=(f\cdot g)\circ g(x)$ represent gray scale opening and gray scale closing of f by structuring element g, respectively. The residual image after filtering is

$$r = f - Hyb(f). \tag{3}$$

The structuring elements are defined by a quadratic structuring function

$$g(x) = -\frac{1}{2\rho}x^T x, \tag{4}$$

where ρ is the size of the structuring element. The image filtering results depend on the size and sometimes the shape of the structuring element.

Motion of an object obeys determinate dynamic rules. The characteristics of motion restrict the object to appearing in an adjacent domain in the succeeding images. Thus, the conjunction function is

$$d(i,j,k) = \min[c \times (f(i+d_i, j+d_j, k) - f(i,j,k-1))], \tag{5}$$

where c is a coefficient, f denotes the intensity of image, i, j are the pixel coordinates in the image, k represents the frame number of image, d_i, d_j denote the adjacent domains of a given pixel, respectively.

Energy Features

Background is often covered with clouds and fogs in real world IR images. The moving objects are always merged with the clouds and influenced by imaging noise, which makes it difficult to detect objects in clouds. In Ref. 6, an imaging model is described as follows:

$$f(x,y,k) = f_T(x,y,k) + f_B(x,y,k) + \eta(x,y,k), \tag{6}$$

where $f(x,y,k)$ represents the intensity of location (x,y) of the kth frame of an IR image, $f_T(x,y,k)$ and $f_B(x,y,k)$ represent the object intensity and background intensity, respectively, and $\eta(x,y,k)$ represents the intensity of the measurement noise.

The energy feature-based object detection method was applied after preprocessing a single frame in an IR image using mathematical gray value morphology, and the background image was estimated accordingly. Then, a new image is obtained as the original image minus the estimated background image. According to the object energy feature of the new image, all possible targets are extracted after target detection processing.

Mathematical morphology operations include four basic operations, namely, erosion, dilation, opening, and closing. In Eq. (2), f denotes the image, which is to be processed, and g denotes the structuring element, which has various patterns. D_f and D_g denote the definition areas of image f and structuring element g, respectively. For the IR images, a 7×7 diamond shape flat structuring element can be adopted.

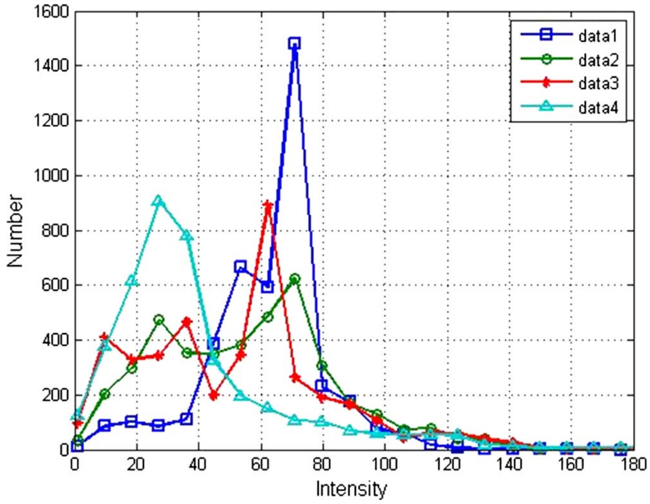

Figure 1. Histogram of objects and backgrounds for the case of an object approaching an IR imaging system.

An energy feature-based method for object detection includes two characteristic values, which are described as follows:[6]

(1) Local energy: the local energy is defined as the summation of areal (5×5) intensity of each pixel of the detection window. $LP_{\max}$ denotes the maximum intensity.
(2) Single point energy: in one of the object plus noise images, the object appears at some pixels where the intensity values are often greater than the intensity values of other pixels. $SP_{\max}$ denotes the single maximum intensity value of the whole image.

Workflow for the possible target location and intensity (noise plus target) is designed as follows:

$$T(i,j) = O(i,j) - B(i,j), \tag{7}$$

where, $T(i,j)$, $O(i,j)$, and $B(i,j)$ are noise plus target image, original image, and estimated background image, respectively. $LP_{\max}$ denotes $\Sigma T(m,n)$ for the maximum of local energy, where $i-2\le m\le i+2$ and $j-2\le n\le j+2$ represent index values, respectively. $SP_{\max}$ denotes $T(m,n)$ for a single point energy (intensity).

Cubic Facet Model

We proposed the facet-based detection scheme for small moving objects with f zero-mean Gaussian noise in previous research.[12] The gray-level intensity surface at each facet is approximated using a bivariate cubic function $f(r,c)$, where r and c denote a row and a column, respectively. For a cubic function $f(r,c)$, the polynomial bases with an order higher than 3 are ignored. The K_m, $m=1,\ldots,10$, are coefficients for the bivariate cubic function $f(r,c)$ expressed in discrete orthogonal polynomials. The coefficient K_m for all m is

$$K_m = \frac{\sum\limits_{(r,c)\in S} I(r,c) g_m(r,c)}{\sum\limits_{(r,c)\in S} [g_m(r,c)]^2}, \tag{8}$$

where S is a symmetric two-dimensional facet defined as $R\times C$, and $I(r,c)$ represents intensity value at $(r,c)\in S$. Likewise, each fitting coefficient K_m can be calculated individually as a linear combination of the intensity values $I(r,c)$. The weight kernel for each $I(r,c)$ for the mth coefficient is

$$W_m = \frac{\sum\limits_{(r,c)\in S} g_m(r,c)}{\sum\limits_{(r,c)\in S} [g_m(r,c)]^2}. \tag{9}$$

For determination of potential object pixels, by the bivariate cubic function $f(r,c)$, the second order partial derivatives at the facet center (0,0) are

$$f_{rr} = \frac{\partial^2 f(r,c)}{\partial r^2} = 2K_4, \quad f_{rc} = \frac{\partial^2 f(r,c)}{\partial r\,\partial c} = K_5, \quad f_{cc} = \frac{\partial^2 f(r,c)}{\partial c^2} = 2K_6. \tag{10}$$

If a pixel is an object, we assume that it is likely to be the maximum extreme point. According to the extreme theory, the following conditions must be satisfied:

$$D_1 = f_{rr} < 0, \quad D_2 = f_{rr} f_{cc} - f_{rc}^2 > 0, \quad D_3 = f_{cc} < 0, \tag{11}$$

where D_1, D_2, and D_3 represent horizontal, diagonal, and vertical extremum values, respectively. Furthermore, the weight kernels for K_4, K_5, and K_6 are

$$W_4 = \frac{1}{70}\begin{bmatrix} 2 & 2 & 2 & 2 & 2 \\ -1 & -1 & -1 & -1 & -1 \\ -2 & -2 & -2 & -2 & -2 \\ -1 & -1 & -1 & -1 & -1 \\ 2 & 2 & 2 & 2 & 2 \end{bmatrix},$$

$$W_5 = \frac{1}{100}\begin{bmatrix} 4 & 2 & 0 & -2 & -4 \\ 2 & 1 & 0 & -1 & -2 \\ 0 & 0 & 0 & 0 & 0 \\ -2 & -1 & 0 & 1 & 2 \\ -4 & -2 & 0 & 2 & 4 \end{bmatrix}, \tag{12}$$

$$W_6 = W_4^T.$$

From the above considerations, the basic object conditions are obtained based on the extreme theory. To reduce the occurrence of false alarm pixels, the conditions mentioned in Eq. (11) need to be modified. We use the conditions presented in by Wang[10] as follows:

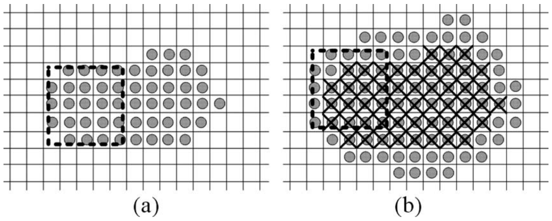

Figure 2. Processing facet-based model for larger moving objects: (a) ($k-1$)th frame and (b) kth frame.

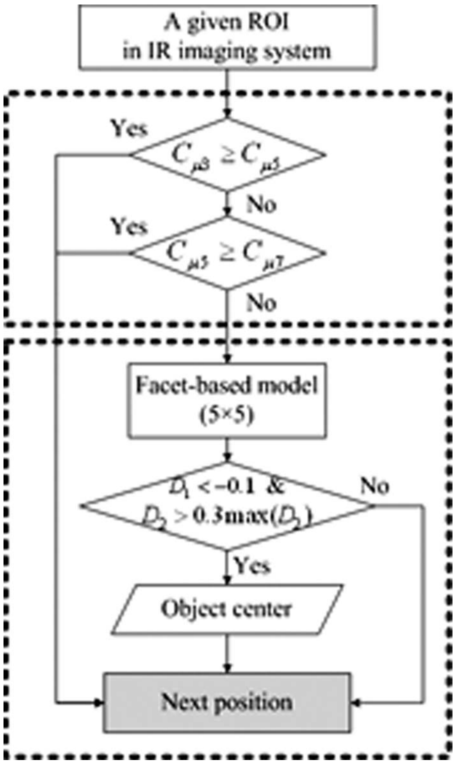

Figure 3. Block diagram of the proposed scheme for larger moving objects.

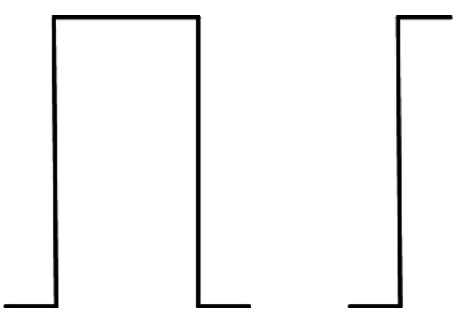

Figure 4. Types of edge in image: (a) line edge and (b) step edge.

$$D_1 < -0.1, \quad D_2 > 0.3\ \max(D_2), \tag{13}$$

where $\max(D_2)$ is the maximum of D_2. The facet-based object detection procedure is described as follows:

1. Obtain D_1 and D_2 in Eq. (11) by calculating K_4, K_5, and K_6 through convolution of the original image with W_4, W_5, and W_6 in Eq. (12), respectively.

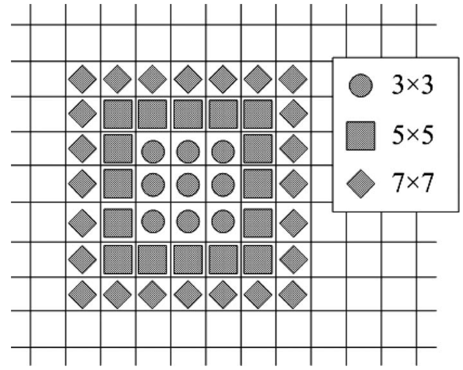

Figure 5. Extraction of mean of image intensity for an expanding moving object.

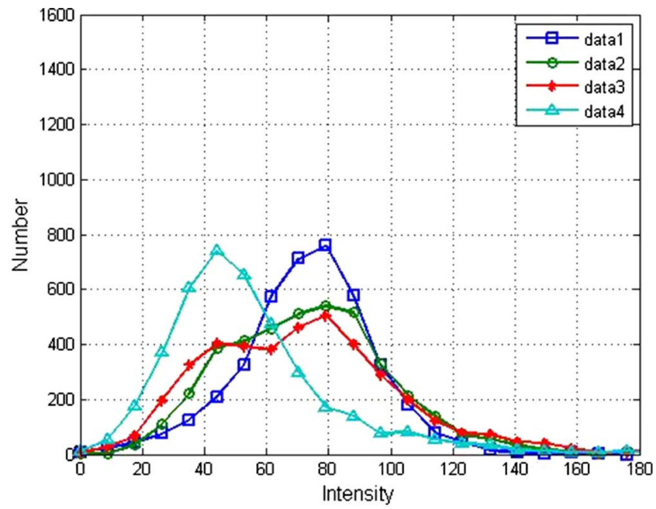

Figure 6. Object and background histogram for the position of the maximum extreme point with Gaussian noise $N(0,5^2)$ for Fig. 1.

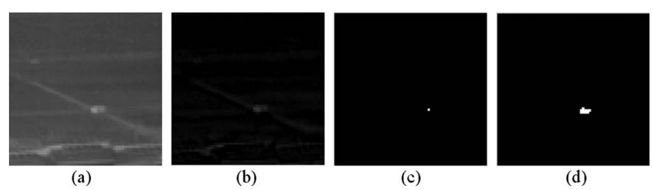

Figure 7. Simulation results for test frame in IR imaging system.

2. Determine whether or not the pixel is an object point using the maximum extremum conditions given in Eq. (13).
3. Repeat steps 1 and 2, decide, and store all the possible object pixels.

ROBUST SCHEME FOR A LARGER OBJECT

The performance of the facet-based detection is affected by larger object size and noise, especially in the case of an object approaching the IR imaging system for the case of zero-mean Gaussian noise. As an object approaches, the IR imaging system occurs differences in object and background intensity between the current information and the previous information that are a consequence of object expansion at the same-positioned pixel and of the object moving on a

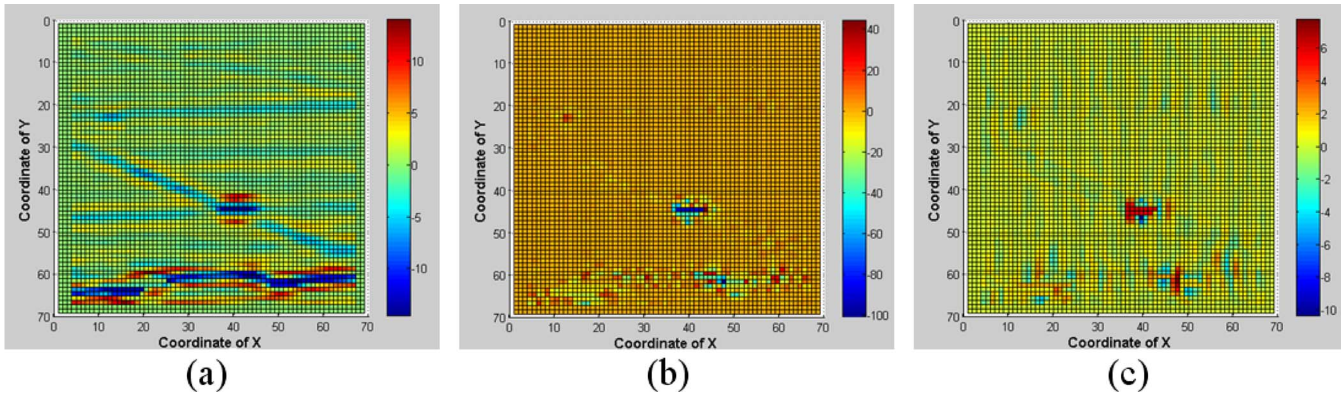

Figure 8. Extremum points for facet-based model object detection: (a) D_1, (b) D_2, and (c) D_3.

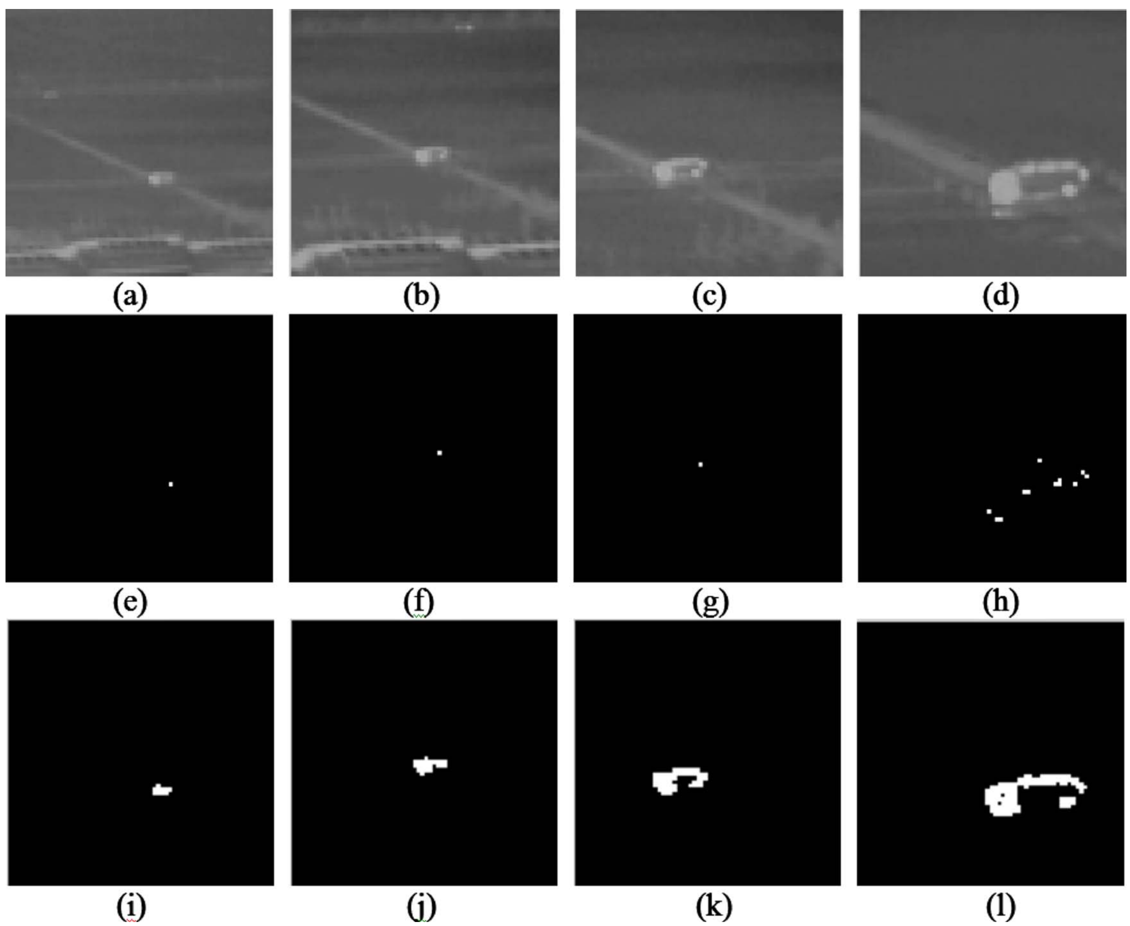

Figure 9. Segmentation results from 43rd to 341st frames: (a)–(d) original image; (e)–(h) facet-based model; and (i)–(l) proposed scheme.

different direction, as shown in Figure 1. In this case, we must change the kernel size limit of the facet-based model, but it is difficult to resize the kernel size for every iteration.

Robust Scheme for Larger Moving Object

To detect the larger object and mitigate the noise effect, various details can be used. Under the assumption that an object is brighter than the background, the size of the object approaching the IR imaging system is larger than the previous object. Let us consider the situation, where an object is moving from the $(k-1)$th frame to the kth frame, as shown in Figure 2. If the object is large and moving, the probability that the difference between the size and intensity of the object pixel in the current frame and that of the same-positioned pixel in the current frame is larger than the object of previous frame. Fig. 2(a) shows an object of $n \times n$ size in the $(k-1)$th frame; Fig. 2(b) shows that the object in the kth frame is now larger than the previous object.

The proposed scheme therefore consists of two stages.

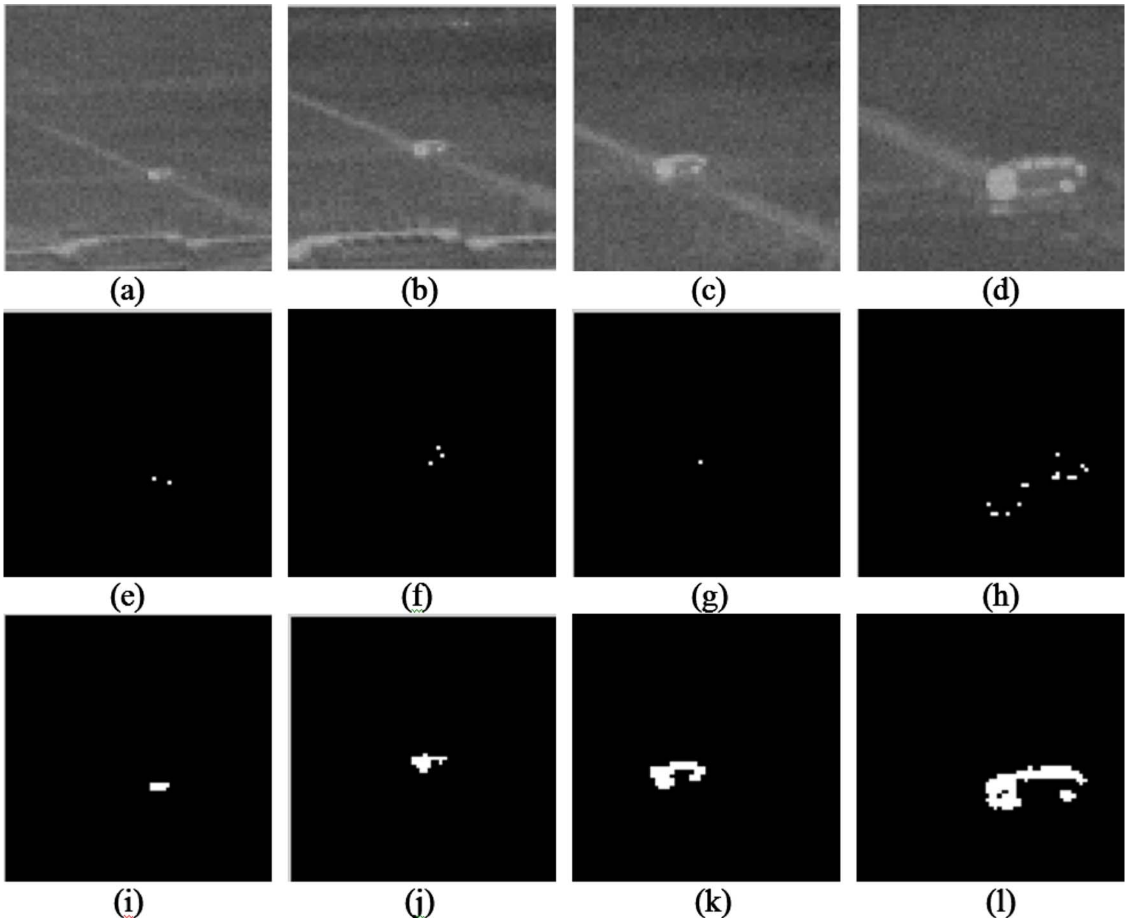

Figure 10. Segmentation results from 43rd to 341st frames with Gaussian noise $N(0,5^2)$: (a)–(d) original image; (e)–(h) facet-based model; and (i)–(l) proposed scheme.

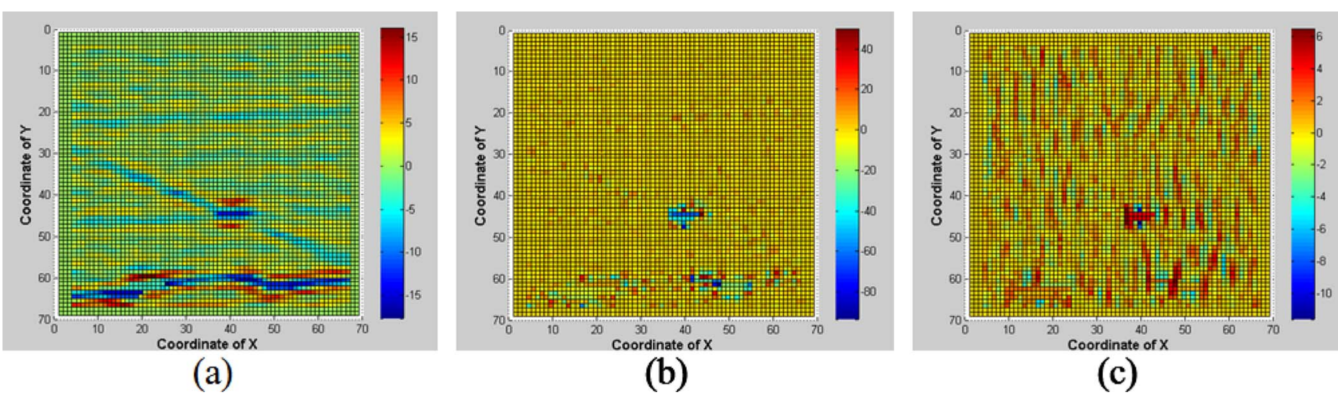

Figure 11. Extremum points for proposed scheme object detection (a) D_1, (b) D_2, and (c) D_3 with Gaussian noise $N(0,5^2)$.

First, we extract a mean of image intensity from the center of the facet in ROI of the current frame. Second, we apply it to the facet-based model in the same-positioned pixel. If the size of the current object is larger than the previous object, it is divided into many objects to which the facet-based model is applied. Thus, a kernel size larger than 5×5 occurs because the facet-based model uses a third order polynomial expression, and it determines the limit of the kernel size. Therefore, we propose a scheme that compares a mean of image intensity for 3×3, 5×5, and 7×7 from the center of the facet-based model kernel. The proposed scheme can extract not only one large object but also many segmented objects. A block diagram of the proposed scheme is shown in Figure 3. In Fig. 3, the first stage is to extract a mean of image intensity in a given ROI of the current frame and the second stage is to process the facet-based model.

An object in the proposed scheme exists as one massive object. This object of this scheme is to find an edge of the

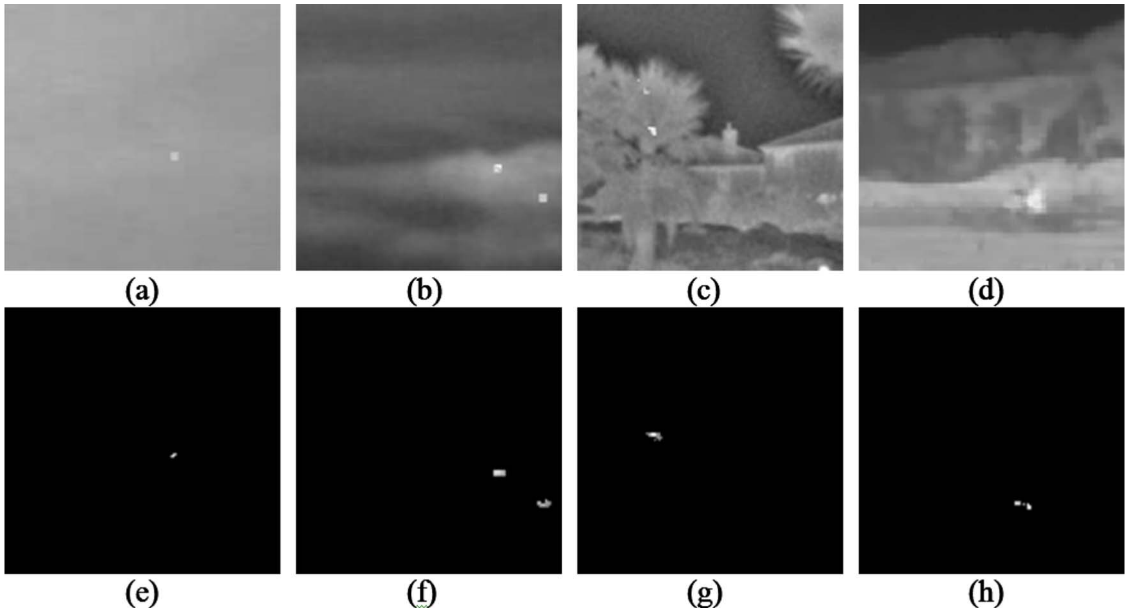

Figure 12. Segmentation results of Sky, Clouds, House, and Mountain: (a)–(d) original image; (e)–(h) the proposed algorithm for different backgrounds.

object. The edge is shown by discontinuous points of pixel intensity which define the boundary of a region in the image. This approach can classify step edge and line edge in the image. Figure 4 shows a step edge that corresponds to discontinuous points and a line edge that corresponds to linear arrayed discontinuous points, respectively. The edge corresponds to information about contours of the object and provides information of object position, shape, size, and surface pattern in an IR image.

We assume that the range of the object size is already known and the size is larger than or equal to 3×3; μ_i is defined as the sample mean in an eight-connection neighborhood of an object for 3×3, 5×5, and 7×7 regions represent the kernel size of the sample mean

$$\mu_i = \frac{\sum_{r=-n}^{n}\sum_{c=-n}^{n} I_i(r,c)}{N}, \tag{14}$$

where r and c represent the values of the region for a row and a column, respectively. N and n represent the size of the region and define $n\times n$, respectively. We extract and compare mean values of intensity for 3×3, 5×5, and 7×7 regions from the center of facet-based model kernel in the larger object (Figure 5). At this time, we apply to Eq. (13) through the segmentation condition of the facet-based model. The next stage decides whether or not the condition for Eq. (14) is satisfied. If the condition is satisfied, we move to the adjacent pixel to which the facet-based model is not currently applied

$$C_{\mu3} \geqslant C_{\mu5},\ C_{\mu5} \geqslant C_{\mu7}, \tag{15}$$

where $C\mu$ represents the sample mean for 3×3, 5×5, and 7×7 regions in an object of current frame.

The performance of the facet-based detection is affected by noise in the IR imaging system, especially zero-mean Gaussian noise. If Gaussian noise occurs in the image, we have shown in our previous research[12] that the facet-based model can robustly detect a small moving object. Let $I_k(r,c)$ be defined as $I(r,c)$ in the kth frame, and $n_k(r,c)$ be defined as Gaussian noise at (r,c) at the kth frame. We assume

$$n_k(r,c) \sim N(0,\sigma_n^2), \tag{16}$$

with $n_k(r,c)$ and $n_l(r,c)$ being independent of each other if $k\neq l$. Gaussian noise can shift the position of the maximum extreme point or make a false maximum extreme point for Fig. 1, as illustrated in Figure 6.

EXPERIMENTAL RESULT

To demonstrate the performance of the proposed algorithm, we simulate a larger object in infrared image sequences. Figure 7(a) is the test frame for an IR imaging system, (b) is the frame difference with standard deviation, (c) is the facet-based model at previous research,[12] and (d) is the proposed algorithm. An object size in Fig. 7 is 3×3. Figure 8 shows extremum values that apply to facet-based model object detection for Fig. 7(a). Fig. 8(a) shows horizontal extremum value D_1, Fig. 8(b) shows diagonal extremum value D_2, and Fig. 8(c) shows vertical extremum value $D_3<0.1$.

Figures 9(a)–9(l) show segmented results of “Cars” from the 43rd to 341st frame by the IR imaging system. Figs. 9(a)–9(d) show the original frame, Figs. 9(e)–9(h) show the result from the facet-based model in previous research,[12] and Figs. 9(i)–9(l) show the result from the proposed scheme. Fig. 9(h) shows segmentation into many objects because of the change in intensity values around object.

Figs. 10(a)–10(l) show segmented results for “Cars” with Gaussian noise $N(0,5^2)$ from the 43rd to 341st frame

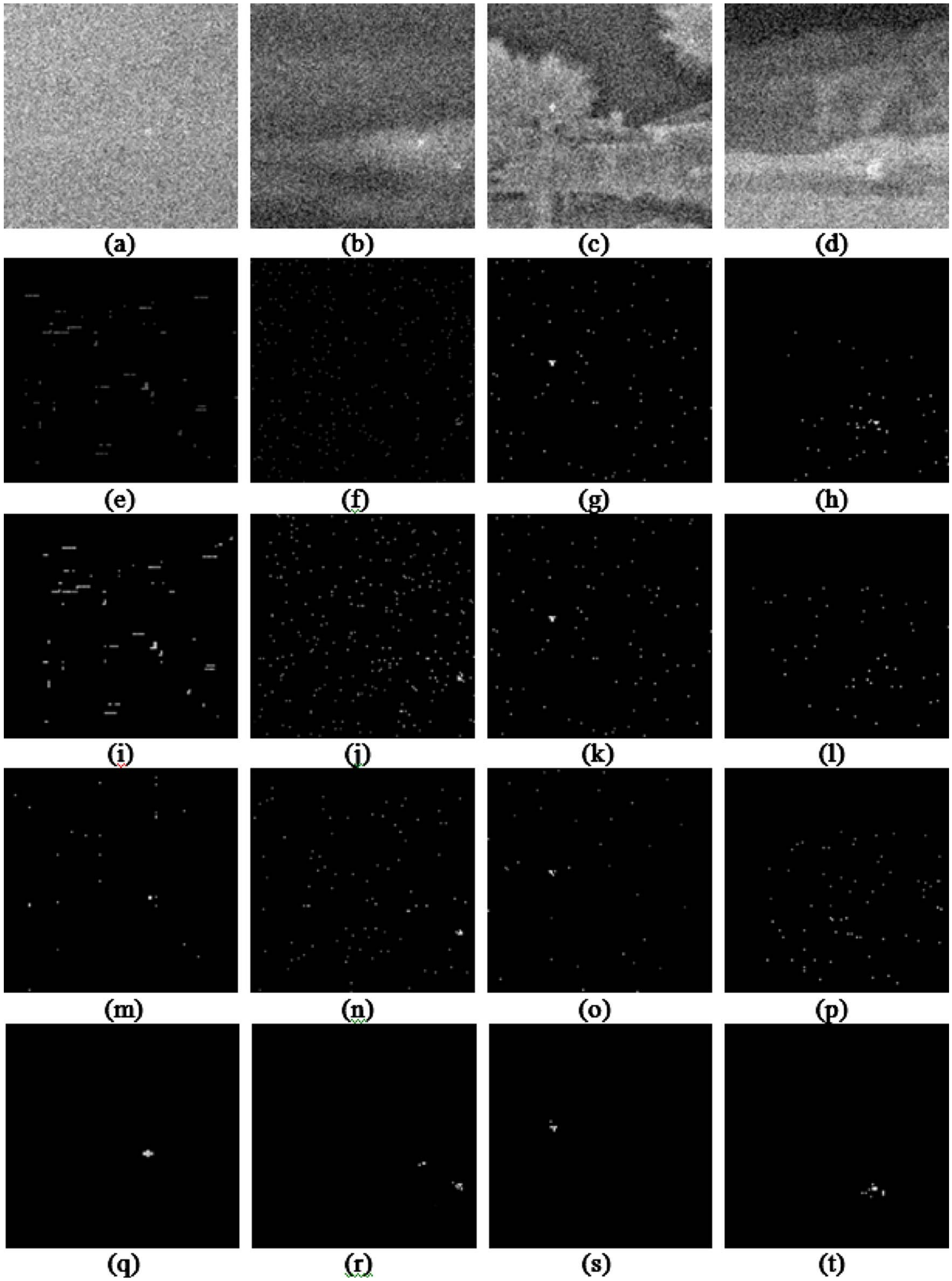

Figure 13. Segmentation results of Sky, Clouds, House, and Mountain: (a)–(d) original image with Gaussian noise $N(0,25^2)$; (e)–(h) TopHat; (i)–(l) image-(opening+closing)/2; (m)–(p) facet-based model; (q)–(t) proposed method.

in Fig. 9. Figs. 10(a)–10(d) show the original frame with Gaussian noise $N(0,5^2)$, Figs. 10(e)–10(h) show the result from the facet-based model in previous research,[12] and Figs. 10(i)–10(l) show the result from the proposed scheme. Fig.10(g) shows only one object for segmentation, but others show multisegmentation because of the change in the extremum points of the intensity values around the object. The proposed scheme shows robustness against Gaussian noise. Figure 11 shows extremum values that apply to the proposed object detection scheme for the first figure in the top row in

Table I. Elapsed time comparison of several small object detection methods.

Detective methods	A	B	C	D	Average time
Image-(opening+closing)/2	43.772	49.660	45.116	57.134	50.921
TopHat	15.575	21.081	15.989	15.733	19.095
Facet-based model	25.566	26.445	24.408	29.696	28.529
Proposed method	22.663	24.293	22.179	26.988	26.031

Fig. 11. Fig. 11(a) shows horizontal extremum value D_1, Fig. 11(b) shows diagonal extremum value D_2, and Fig. 11(c) shows vertical extremum value D_3.

For these experiments, we select a typical infrared 128×128 image sequence from many images for a small moving object. Figures 12(a)–12(d) show the segmentation results for 37th frame of "Sky," 22nd frame of "Clouds," 15th frame of "House," and 16th frame of "Mountain." Figs.12(e)–12(h) show the results obtained by using the proposed algorithm with different backgrounds, in the experiments the kernel size $(R\times C)$ is 5×5 pixels.

Figures 13(a)–13(d) show noise images with Gaussian noise $N(0,25^2)$ from the original image of Figs. 12, Figs. 13(e)–13(h) show the results from Image (opening +closing)/2, Figs. 13(i)–13(l) show the results using TopHat, and Figs. 13(m)–13(t) show the results obtained with the facet-based algorithm and the proposed algorithm, respectively.

The experimental data are listed in Table I, which shows that the filtering performances of several filters for the 128×128 size images with different backgrounds corresponding to Fig. 13. In the image-(opening+closing)/2 and TopHat, a 3×3 pixel kernel was used. In the facet-based algorithm and the proposed algorithm, a 5×5 pixel kernel was used. It is obvious that the TopHat method demands minimum time consumption for small object detection with different backgrounds, but we also show the results yielded more false alarm points than the proposed algorithm. The TopHat algorithm needs a method of elimination of background clutter for the final target decision.

CONCLUSION

In this article, a robust detection scheme using the facet-based model for a larger moving object in the infrared is proposed. We also proposed a new condition in the facet-based expanding object detection algorithm for the case of zero-mean Gaussian noise because it is difficult to detect a larger moving object using the current facet-based model, given the kernel size of 5×5 pixels. The difference between size and intensity of the object pixel in the current frame and those of the same-positioned pixel in the previous frame shows that the object in the current frame is larger than the object in the previous frame. Incorporating the facet-based detection scheme, the proposed algorithm can eliminate false alarm points for an expanding moving object. In the proposed algorithm, the pixels are detected from the maximum extreme condition. The experimental results show that the proposed algorithm is efficient and robust.

REFERENCES

[1] J. Wang, J. Chun, and Y. Park, "Adaptive matched filtering for the varying attitude of a target", Proc. SPIE **3968**(22), 1–9 (2000).

[2] X. Cai, Y. Hu, G. Hu, X. Tao, and W. Lei, "Morphology based adaptive preprocessing method of infrared image sequence", Proc. SPIE **6279**, 1–7 (2007).

[3] Y. Wang, T. Zhang, and G. Wang, "Small-target predetection with an attention mechanism", Opt. Eng. **41**(4), 872–885 (2002).

[4] X. Huang and J. Zhang, "Detection of small target in infrared images based on multi-band background model", Proc. SPIE **5640**, 350–357 (2005).

[5] N. Dong, G. Jin, B. Oi, and J. Ma, "New approach to detect dim moving point targets based on motion analysis", Proc. SPIE **4473**, 34–42 (2001).

[6] S. Zhang, Z. Jing, J. Li, and H. Leung, "Small target detection of infrared image based on energy features", *Proc. IEEE International Conference on Neural Networks and Signal Processing* (IEEE, Piscataway, NJ, 2003) Vol. **1**, pp. 672–676.

[7] L. Yang, J. Yang, and K. Yang, "Infrared background suppression for segmenting and detecting small target", Electron. Lett. **40**, 1083–1085 (2004).

[8] H. Sang, C. Chen, and X. Shen, "Structural parameter of TDNLMS adaptive prediction filter used in point objects detection in digital image data", J. Huazhong Univ. Sci. Technol., **31**(1), 58–60 (2003).

[9] S. Zheng, C. Xiong, J. Tian, and J. Liu, "One efficient facet-based small target detection technique", *Proc. IEEE International Conference on Signal Processing* (IEEE, Piscataway, NJ, 2004), Vol. **1**, pp. 885–888.

[10] G. Wang, C. Chen, and X. Shen, "Facet-based infrared small target detection method", Electron. Lett. **41**(22), 1244–1246 (2005).

[11] R. Haralick, "Digital step edges from zero crossing of second directional derivatives", IEEE Trans. Pattern Anal. Mach. Intell. **6**(1), 58–68 (1984).

[12] H. Lee, S. Kim, D. Park, J. Kim, and C. Park, "Robust method for detecting an infrared small moving target based on the facet-based model", Proc. SPIE **6969**, 1–9 (2008).